Determinants of Sequence-Specific DNA Methylation: Target Recognition and Catalysis Are Coupled in M.HhaI†

Ben Youngblood,‡ Fabian Buller,‡,§ and Norbert O. Reich*

Department of Chemistry and Biochemistry and Program in Biomolecular Science and Engineering, University of California, Santa Barbara, California 93106-9510

Received July 13, 2006; Revised Manuscript Received October 21, 2006

ABSTRACT: Sequence specificity studies of the wild-type bacterial DNA cytosine C^5 methyltransferase HhaI were carried out with cognate (5′GCGC3′) and noncognate DNA substrates containing single base pair changes at the first and the fourth position (underlined). Specificity for noncognate site methylation at the level of k_{cat}/K_D^{DNA} is decreased 9000−80000-fold relative to the cognate site, manifested through changes in methylation, or a prior step, and changes in K_D^{DNA}. Analysis of a new high-resolution enzyme−DNA cocrystal structure provides a partial mechanistic understanding of this discrimination. To probe the significance of conformational transitions occurring prior to catalysis in determining specificity, we analyzed the double mutant (H127A/T132A). These amino acid substitutions disrupt the interface between the flexible loop (residues 80−99), which interacts with the DNA minor groove, and the active site. The mutant's methylation of the cognate site is essentially unchanged, yet its methylation of noncognate sites is decreased up to 460-fold relative to the wild-type enzyme. We suggest that a significant contribution to M.HhaI's specificity involves the stabilization of reaction intermediates prior to methyl transfer, mediated by DNA minor groove−protein flexible loop interactions.

DNA-modifying enzymes recognize their target sequence in multiple ways, including direct readout of DNA bases and indirect readout of sequence-dependent conformational features (*1*). Our understanding of the relative energetic contributions of these and other interactions toward specificity is incomplete in spite of extensive efforts to reengineer such enzymes (*2*−*4*) or develop semisynthetic approaches toward the same ends (*5*−*7*). Evidence that direct and indirect interactions alter both the stability and interconversion of reaction intermediates prior to the Michaelis complex (*8*−*11*) suggests a plausible mechanism relating such interactions directly to enzyme specificity. DNA methyltransferases provide an excellent opportunity to investigate the molecular basis of enzyme specificity: these enzymes are key players in epigenetic processes such as genetic imprinting, mismatch repair, host defense, and gene regulation, and they recognize and modify specific 2−6 base pair sequences using the same cofactor *S*-adenosyl-L-methionine (AdoMet) (*12*). The highly conserved nature of the protein sequences and structural organization of the DNA cytosine methyltransferases suggest that investigations of M.HhaI, the target enzyme of our investigation, may be relevant for other members of this broad class of enzymes, as well as other enzymes that exploit similar mechanisms (base flipping, methyl transfer to pyrimidines, modification of specific sites within DNA) (*13*, *14*).

The two-domain organization of AdoMet-dependent methyltransferases is revealed by the superimposed binary and ternary structures of the DNA cytosine C^5 methyltransferase M.HhaI (Figure 1A) (*13*). The larger domain is highly conserved among DNA C^5 methyltransferases and contains the active site and the binding pocket for AdoMet (*13*). The less conserved small domain is believed to be involved in target recognition, although contributions to substrate discrimination involving the large domain have also been suggested (*15*, *16*).

Further comparison between the binary and ternary cocrystal structures of M.HhaI reveals that, upon binding cognate DNA, the small domain closes around the target sequence along with the ∼26 Å movement of a flexible loop (Figure 1A); this loop interacts with the minor groove, and the conformations of several active site residues are directly and indirectly altered by this loop motion. Binding of nonspecific DNA by M.HhaI does not induce the same loop motion (Estabrook and Reich, in press) (*17*). DNA methylation requires the stabilization of the target cytosine into the active site adjacent to AdoMet and the active site nucleophile Cys81, which resides in the flexible loop. This extrahelical repositioning of the target base is frequently referred to as base flipping (*15*).

In vitro specificity studies of DNA methyltransferases have focused largely on specific protein residues and their impact on target recognition, examined by mutational analysis; a small number of studies have described the discrimination with noncognate substrates (*9*, *18*−*23*). Here we describe a quantitative analysis of M.HhaI specificity, initially probed with six single-site-modified DNA sequences (Figure 1B)

† This work was supported by NSF Grant MCB-9983125 and NIH Grant RO1GM053763-08A2. This work was also partially funded through a scholarship from the Dr. Peter Schaefer Program for Sustainable Development, awarded to F.B.

* To whom correspondence should be addressed: e-mail, reich@chem.ucsb.edu; tel, 805-893-8368.

‡ These authors contributed equally to this work.

§ Visiting student from the Institut für Biochemie, Westfälische Wilhelms-Universität, D-48149 Münster, Germany.

10.1021/bi061414t CCC: $33.50
Published on Web 12/06/2006

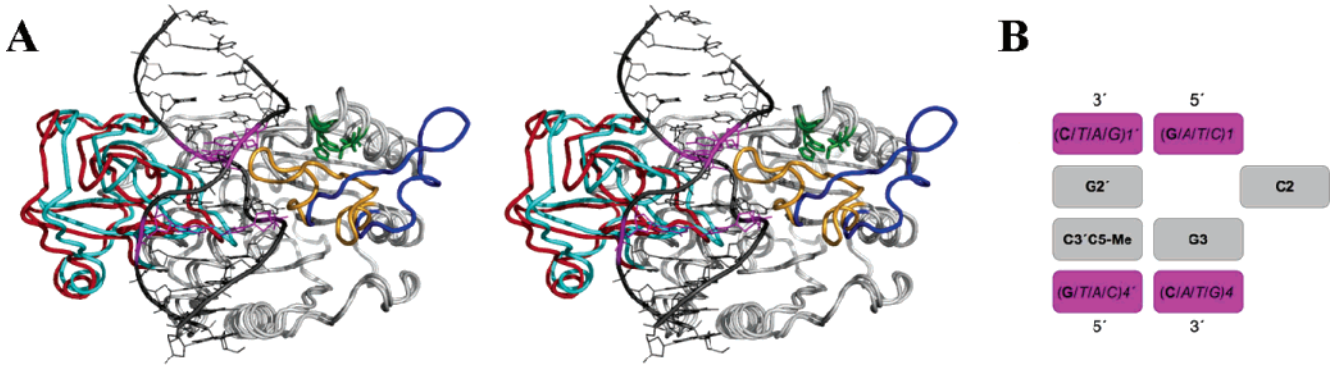

FIGURE 1: Structural and schematic view of M.HhaI and the DNA substrate(s). (A) Stereoview of superimposed M.HhaI structures unbound (PDB ID 1HMY) and bound (PDB ID 3MHT) to DNA. The binary and ternary structures were superimposed using backbone atoms (residues 1−180), minus the flexible loop backbone, with an RMSD of 0.56 Å. The flexible loop (residues 80−99) moves ~26 Å (Cα Lys89 to Cα Lys89) from the open conformation (blue) to the closed conformation (yellow) upon binding cognate DNA. The small domain (amino acids 194−275; red colored, unbound structure; cyan colored, bound structure) (*24*) moves ~2 Å toward the DNA (mean of the distances Cα Gln237 to Cα Gln237, Cα Arg240 to Cα Arg240 and Cα Gly257 to Cα Gly257). Residues His127 and Thr132 (dark green) are above the flexible loop in the closed confirmation. The cofactor has been omitted for clarity. This figure and subsequent figures were created with PyMOL (http://pymol.sourceforge.net/); superimpositions were performed using the program DeepView/Swiss-Pdb View3.7 (*62*). (B) Schematic of the recognition sequence. The flipped cytosine is shifted, base pairs 1 and 4 are colored magenta in panels A and B, substitutions at base pairs 1 and 4 are italicized, and correct bases are in bold.

and compared to the methylation of the cognate site by the wild-type enzyme. This functional analysis can be directly compared to the detailed structural studies of this enzyme (*15*, *24*−*27*). Furthermore, we extended this specificity approach to a double mutant engineered to disrupt the interface between the enzyme's flexible loop and active site (Figure 1A); this interface was previously implicated as a specificity determinant (*28*). The double mutant is significantly more discriminating than the wild-type enzyme, caused largely by a decrease in noncognate site methylation. These results provide molecular insights into how the protein−DNA interface is coupled to the correct assembly of the enzyme's active site, leading directly to an induced fit mechanism.

MATERIALS AND METHODS

Materials. Oligodeoxynucleotides were purchased from Midland Certified Reagent Co. (Midland, TX). Oligodeoxynucleotides were further purified on a Vydac HPLC column (Table 1). To form 100 μM double-stranded substrates, complementary single-stranded oligodeoxynucleotides were mixed at a 1:1 ratio in STE (10 mM NaCl, 10 mM Tris-HCl, pH 7.5, and 1 mM EDTA), heated to 95 °C, and then slowly cooled to room temperature. The annealed substrates were analyzed on a 10% polyacrylamide gel and determined to be >95% double-stranded substrate.

Protein Expression and Purification. WT and the double mutant H127A/T132A M.HhaI were expressed from the vector pHSHW-5 in *Escherichia coli* strain ER1727 and purified as described previously (*29*). Briefly, 8 L of culture was induced with 1 mM isopropyl β-D-thiogalactoside (IPTG) at an OD_{600nm} of 0.4 for 3 h. Cells were spun down, resuspended in phosphate extraction buffer (200 mM NaCl, 6.5 mM K_2HPO_4, 3.5 mM KH_2PO_4, 1 mM EDTA, 7 mM BME, and 1 mM PMSF), and lysed by sonication. The lysate was centrifuged (1 h at 20800*g* in a SA-600 Sorvall rotor at 4 °C), and the supernatant was loaded onto a 25 mL phosphocellulose (Whatman) column. The protein was eluted with a salt gradient between 200 and 800 mM NaCl. Fractions containing the enzyme were further purified using a 10 mL hydroxyapatite (Bio-Rad) column. Protein was eluted with a buffer gradient of 6.5 mM to 1 M potassium phosphate (pH 7.0) also containing 1 mM EDTA and 7 mM β-mercaptoethanol and then dialyzed overnight in extraction buffer containing 10% glycerol. The dialyzed protein was additionally purified on a Bio-Rex column (Bio-Rad) using a salt gradient of 200 to 800 mM NaCl in buffer containing 10% (V/V) glycerol, 10 mM potassium phosphate (pH = 6.8), 1 mM EDTA, and 7 mM β-mercaptoethanol. This procedure leads typically to a purity of greater than 95% as determined by densitometry of sodium dodecyl sulfate−polyacrylamide gel electrophoreses stained with Coomassie.

Table 1: Sequences of DNA Substrates

sequence[a]	substitution[b]	abbreviation
5′-GGGAATTCATG-GCGC-AGTGGGTGGATCCAG-3′		cog
5′-GGGAATTCATT-GCGC-AGTGGGTGGATCCAG-3′		cog2
5′-GGGAATTCATG-ACGC-AGTGGGTGGATCCAG-3′	G1 → A1 hemimethylated	A1
5′-GGGAATTCATG-TCGC-AGTGGGTGGATCCAG-3′	G1→ T1 hemimethylated	T1
5′-GGGAATTCATT-CCGC-AGTGGGTGGATCCAG-3′	G1→ C1 hemimethylated	C1
5′-GGGAATTCATG-GCGA-AGTGGGTGGATCCAG-3′	C4 → A4 hemimethylated	A4
5′-GGGAATTCATG-GCGT-AGTGGGTGGATCCAG-3′	C4 → T4 hemimethylated	T4
5′-GGGAATTCATT-GCGG-AGTGGGTGGATCCAG-3′	C4 → G4 hemimethylated	G4
5′-GGGAATTCATG-ACGC-AGTGGGTGGATCCAGTT-fluor-3′	A1, TT-fluorescein	A1F

[a] The target recognition sequence is underlined. All complement sequences (not shown) form duplex substrates. [b] Hemimethylated = complement strand C3′ (Figure 1B) methylated at the C5 position.

Enzymes were stored at −80 °C in 10% (v/v) glycerol, 0.4−0.5 M NaCl, 10 mM potassium phosphate (pH = 6.8), 1 M EDTA, and 7 mM BME.

DNA Affinity (Gel Mobility Shift Assays). DNA affinity studies were performed as previously reported (*29*). DNA substrates were radiolabeled using [γ-^{32}P]ATP (Amersham Pharmacia Biotech) and T4 polynucleotide kinase (NEB). Electrophoretic gel mobility shift assays were performed with 1−2.5 nM radiolabeled DNA and increasing enzyme concentrations. DNA, enzyme, and 6 μM *S*-adenosyl-L-homocysteine (AdoHcy) (purchased from Sigma) were incubated at room temperature in methylation buffer for 10 min before being loaded onto the gel. Densitometry of shifted bands was analyzed on a Storm 840 phosphorimager with the program ImageQuant (Molecular Dynamics, Amersham Biosciences, Piscataway, NJ). Data were fit to a rectangular hyperbola using the program SigmaPlot. AdoHcy is used as a substrate analogue for the cofactor AdoMet.

DNA Affinity (Fluorescence Polarization Anisotropy). DNA affinity studies using fluorescence polarization anisotropy were performed on substrate A1 with WT and H127A/T132A M.HhaI (*30*, *31*). Fluorescein-labeled duplex oligonucleotide (20 nM), 2 μM AdoHcy, and methylation reaction buffer (500 μL total volume) were combined in a reduced volume quartz cuvette, 10 mm × 4 mm. Aliquots of 2 μL with increasing concentrations of enzyme were added to the reaction mixture to minimize volume changes. Data were collected on a Fluoromax-2 fluorometer (Horiba Jobin Yvon Inc., Edison, NJ) equipped with an L-Format autopolarizer. The polarizer was aligned using a solution of 2 mg/mL glycogen. Polarization and anisotropy values of fluorescein were measured by exciting at 494 nm and measuring an emission at 518 nm. The excitation and emission bandpass was set to 8 nm. The dissociation constant (K_D^{DNA}) was determined by fitting the data to a modified quadratic function using the program SigmaPlot.

Methyl Transfer Assays. As previously described (*29*), the incorporation of tritium-labeled methyl groups into DNA was monitored by a filter binding assay. Reaction buffer, protein dilution buffer, DE81 filter papers, and sample processing were performed as previously described (*29*). *S*-Adenosyl-L-methionine (AdoMet) was purchased from Sigma-Aldrich and *S*-[*methyl*-^{3}H]adenosyl-L-methionine was purchased from Amersham Biosciences. The steady-state rate constants are apparent rate constants. Time course assays were performed at 37 °C. The reactions were started by adding enzyme to the methylation reaction buffer (100 mM Tris-HCl, pH 8.0, 10 mM EDTA, 10 mM DTT) in the presence of saturating DNA (2−6 μM) and [*methyl*-^{3}H]AdoMet (5.5 μM). The assay time was varied between 5 min and 3 h, and the final enzyme concentrations ranged from 20 to 400 nM. Values for k_{cat} were obtained by dividing the slope of the linear fit by the concentration of the enzyme.

Single-Turnover Analysis. As previously described (*29*, *32*, *33*), time course assays were performed at 37 °C. The reactions were initiated by adding enzyme to the mixture of methylation reaction buffer, DNA substrate, and [*methyl*-^{3}H]AdoMet (5.5 μM). The final DNA concentration was 500 nM and final enzyme concentration was 4 μM. The reaction was quenched at varying time points with sodium dodecyl sulfate and spotted on DE81 filter paper. Time points for quenching the single-turnover assays ranged from 0 to 35 min for noncognate substrates. Values for k_{chem} were obtained by fitting the data to a single exponential equation.

Steady-State Kinetic Analysis. As previously described (*29*, *32*, *33*), the constants K_M^{DNA} were measured by a titration of DNA from 50 nM to 20 μM, using saturating concentrations of the cofactor. Depending on the observed activity, reaction times were varied between 30 min and 1 h, and the final enzyme concentration was varied between 20 and 100 nM. Values for K_M^{DNA} were obtained by fitting the data to a rectangular hyperbola using the program SigmaPlot.

RESULTS

k_{cat}/K_M^{DNA} Specificity Constants for WT M.HhaI. In spite of extensive mutational and structural studies, no comprehensive specificity study involving M.HhaI has been reported. Here we describe M.HhaI's specificity at the level of k_{cat}/K_M^{DNA} using cognate and six noncognate synthetic substrates. The noncognate double-stranded DNA substrates have a single-site substitution in the first or fourth base pair of the target recognition sequence 5′-GCGC-3′ (Figure 1B and Table 1). Hemimethylated substrates were used to ensure a single functional binding orientation of the enzyme (*22*). As a control, two substrates with the cognate sequence (cog) and a different flanking sequence (cog2) were used, and the catalytic rates were found to be independent of the 5′ flanking nucleotide (data not shown). The unmethylated cognate substrate was selected for comparison to the hemimethylated noncognate substrate rather than the hemimethylated cognate substrate since gel mobility shift assays with hemimethylated cognate substrate produce two shifted bands, leading to a convoluted interpretation of K_D^{DNA} comparisons (Youngblood and Reich, unpublished observation). Furthermore, because the unmethylated cognate substrate was used with both WT and the double mutant, this specificity comparison is normalized. The modified substrates were divided into those containing substitutions at guanine 1 (base pair 1) and those containing substitutions at cytosine 4 (base pair 4) (Figure 1B and Table 1).

The catalytic turnover constants (k_{cat}) for the noncognate substrates are at least 40-fold slower relative to the cognate substrate (Table 2 and Figure 2A). The K_M^{DNA} values for noncognate substrates are increased up to 420-fold compared to the cognate site (Table 2). K_M^{DNA} includes all kinetic parameters involved in DNA binding, base flipping, and methyl transfer (*33*). k_{cat}/K_M^{DNA} represents the ability of the free enzyme and DNA to attain the transition state (*22*, *34*) and provides a measure of the enzyme's specificity for a particular substrate.

k_{cat}/K_D^{DNA} Specificity Constants for WT M.HhaI. Specificity comparisons relying on k_{chem}/K_D^{DNA} are potentially more readily interpreted in the context of the available enzyme−DNA cocrystal structures, since the K_D^{DNA} term is limited to steps up to and including the tight binding complex. The use of k_{chem} vs k_{cat} allows for the examination of intermediates leading up to the chemistry step and their roles in discrimination, whereas k_{cat} incorporates steps following chemistry such as product release, which in the case of M.HhaI dominates k_{cat} (*22*, *29*). Since methyl transfer is followed by a rate-limiting product release step, WT M.HhaI has a kinetic burst of product formation with cognate DNA under conditions of relatively high enzyme concentrations (*21*, *29*). WT

Table 2: WT M.HhaI Kinetic and Thermodynamic Constants

	sequence[a]	k_{cat} (s^{-1})[e]	K_M (nM)	k_{cat}/K_M ($s^{-1}M^{-1}$)	K_D (nM)	k_{chem} (s^{-1})	k_{cat}/K_D ($s^{-1}M^{-1}$)
cog	GCGC[b]	$8.5 \times 10^{-2} \pm 5.0 \times 10^{-3}$	4.0 ± 0.7	2.1×10^{7}	0.2 ± 0.16	0.14 ± 0.02	7.0×10^{8} [d]
A1	**A**CGC[c]	$2.1 \times 10^{-3} \pm 9.0 \times 10^{-5}$	280 ± 65	7.5×10^{3}	60 ± 5.7	$1.1 \times 10^{-2} \pm 9.0 \times 10^{-4}$	3.5×10^{4}
T1	**T**CGC	$8.2 \times 10^{-4} \pm 3.2 \times 10^{-5}$	770 ± 84	1.1×10^{3}	41 ± 6.8	$7.0 \times 10^{-4} \pm 2.0 \times 10^{-4}$	2.0×10^{4}
C1	**C**CGC	$2.2 \times 10^{-3} \pm 1.0 \times 10^{-4}$	630 ± 66	3.5×10^{3}	28 ± 19	$2.0 \times 10^{-3} \pm 2.0 \times 10^{-4}$	7.6×10^{4}
A4	GCG**A**	$3.3 \times 10^{-4} \pm 2.9 \times 10^{-5}$	560 ± 78	5.9×10^{2}	12 ± 7.4	$3.0 \times 10^{-4} \pm 2.0 \times 10^{-4}$	2.8×10^{4}
T4	GCG**T**	$4.5 \times 10^{-4} \pm 2.7 \times 10^{-5}$	1700 ± 300	2.6×10^{2}	50 ± 5.2	$8.0 \times 10^{-4} \pm 1.0 \times 10^{-4}$	9.0×10^{3}
G4	GCG**G**	$5.5 \times 10^{-4} \pm 1.0 \times 10^{-4}$	390 ± 130	1.4×10^{3}	71 ± 9.1	$3.8 \times 10^{-3} \pm 8.0 \times 10^{-4}$	7.7×10^{3}

[a] 30mer noncognate hemimethylated DNA. [b] Previously reported by Lindstrom et al. (*29*), unmethylated 30mer; $k_{chem} = 0.14 \pm 0.02\ s^{-1}$. [c] K_D^{DNA} by fluorescence anisotropy = 140 ± 10 nM for only noncognate T1; all other K_D^{DNA} values were determined by gel-shift analysis. [d] k_{chem} rate used to determine value. [e] k_{cat} values from the burst assay are within 2-fold of the k_{cat} values calculated from the V_{max} determined in K_M studies.

M.HhaI with noncognate substrates has a diminished burst; thus, a step prior to product release has become rate limiting (Figure 2A) (*28*). Methyl transfer rate constants (k_{chem}) for noncognate substrates, as determined by single-turnover experiments, (Table 2) are the same as the steady-state rate constants (k_{cat}), indicating that indeed the methyl transfer step or a prior step, such as flipping, is rate limiting. To ensure that the DNA is saturated with enzyme, single-turnover experiments were performed with 500 nM DNA and 4 μM enzyme, both concentrations well above the measured affinities of the WT enzyme for all noncognate substrates (Table 2). Therefore, the rate of methyl transfer determined by time course assays was used in calculating the specificity constant k_{cat}/K_D^{DNA}.

To relate our studies to the available crystal structures (*15*, *24*), we measured the dissociation constants of the enzyme with noncognate DNA substrates in the presence of the cofactor AdoHcy. Dissociation constants were measured first by the traditional gel mobility shift assay (*22*, *29*, *35*). Some of the DNA affinities were quite weak, which motivated us to seek an independent measure of this parameter. We therefore developed an anisotropy-based solution assay of DNA binding for M.HhaI (*36*−*38*). Changes in anisotropy result from a change in the rotational diffusion of the fluorophore; therefore, the anisotropy of a fluorophore attached to the substrate DNA is a measure of the enzyme−DNA binding event (*31*). We obtained similar K_D^{DNA} values for A1 using both the gel mobility shift analysis and fluorescence anisotropy measurements, thus validating the use of the gel mobility shift analysis with high nanomolar concentrations of enzyme (Table 1 and Figure 2B). The dissociation constants (K_D^{DNA}) of the ternary DNA−enzyme−AdoHcy complex of WT M.HhaI for noncognate sites determined by the gel mobility shift assay are increased 60−350-fold compared to the cognate site (Table 1 and Figure 2B) (*29*). The shifted DNA−enzyme−AdoHcy band for all noncognate substrates was a smear, suggesting that the dissociation kinetics are increased (*28*). The decreased DNA affinity as well as the decreased rate of methyl transfer observed with M.HhaI for noncognate substrates contributes to the lower specificity for noncognate substrates at the level of k_{cat}/K_D^{DNA} (Figure 2C and Table 2).

H127A/T132A M.HhaI Specificity Study. The coupling of sequence recognition to catalytic efficiency (Table 2) suggests that M.HhaI uses an induced fit mechanism (*15*). The molecular basis of an induced fit mechanism is potentially complex and difficult to assign (*10*, *34*, *38*). One structural element which may contribute to such a mechanism in M.HhaI involves the flexible loop and its interface with the large domain; this loop contacts both the DNA minor groove and the enzyme's active site. Mutations within this interface destabilize the loop and significantly change the enzyme's specificity (*28*). A qualitative analysis of H127A/T132A M.HhaI showed this mutant to have an 18-fold increased discrimination against the noncognate sequence A1 (Figure 2C), without significant changes in AdoMet binding or methylation of the cognate site. We sought to further characterize this mutant with the noncognates used to characterize the WT enzyme to better understand how the flexible loop contributes to M.HhaI's induced fit mechanism.

Like the WT enzyme, H127A/T132A M.HhaI also exhibits a diminished burst magnitude with noncognate substrates compared to the cognate substrate, suggesting that the rate of methyl transfer or a prior step to methyl transfer is rate limiting (Figure 2A). The rate of methyl transfer for noncognate substrates is decreased compared to the cognate substrate 1800−12000-fold for substitutions in base pair 1 and 18000−40000-fold for substitutions in base pair 4 (Table 3). H127A/T132A M.HhaI's rate of methylation is 32−180-fold slower than the WT enzyme for the same noncognate substrates, whereas the rate of methylation of the cognate sequence by each enzyme differs by only 1.2-fold (Tables 1 and 2 and Figure 2A). Due to the very low activity of the mutant toward the noncognate substrates, K_M^{DNA} values were not measured. Noncognate DNA affinity of the H127A/T132A M.HhaI mutant in the presence of the cofactor analogue AdoHcy, as measured by anisotropy and gel mobility shift assays, is decreased 70−500-fold compared to the cognate site (Table 3).

Specificity Enhancement. The stability of reaction intermediates prior to formation of the final catalytic complex is important for M.HhaI's specificity (*28*, *39*). The reaction intermediate in which the target base is positioned extrahelically prior to catalysis is of particular importance (*28*). Destabilization of this intermediate by disruption of the interface between the active site and a highly flexible loop results in changes in base flipping and specificity. The amino acid changes within H127A/T132A M.HhaI are located ~13 Å from the target base and ~12 Å from base pairs 1 and 4, as determined by the two closest atoms of the DNA bases and the residues of the enzyme. Figure 2C shows that substrates T1 and C1 have the most dramatic enhancement of 340- and 460-fold, respectively, compared to WT M.HhaI. Substrates A1, T4, and G4 show enhancements of 18-, 59-, and 30-fold, respectively.

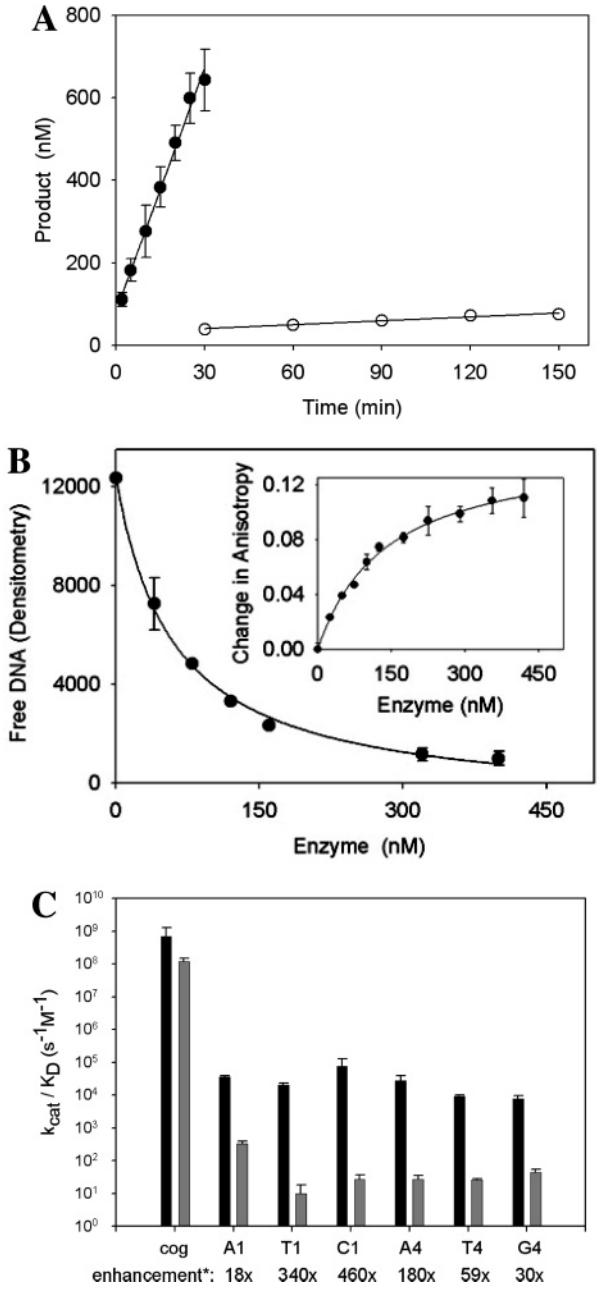

FIGURE 2: Kinetic and thermodynamic analysis of WT and H127A/T132A M.HhaI with cognate and noncognate substrates. (A) Burst analysis of M.HhaI: WT M.HhaI, 400 nM (closed circle), and H127A/T132A M.HhaI, 400 nM (open circle), with 3 μM noncognate substrate T4. Error bars from triplicate experiments are shown. (B) Equilibrium binding of the M.HhaI−DNA−AdoHcy complex. Data were derived from gel mobility shift assays. Densitometry of free noncognate A1 DNA substrate was at 1 nM as a function of WT M.HhaI concentration. Error bars are from duplicate experiments. Data were fit to a rectangular hyperbola yielding a K_D^{DNA} of 60 nM. Inset: Data were derived from fluorescence anisotropy measurements, increasing WT concentration with fluorescein-labeled A1 substrate (20 nM). Data were fit to a modified quadratic function yielding a K_D^{DNA} of 140 nM. (C) The bar diagram shows the specificity constants k_{cat}/K_D^{DNA} on a logarithmic scale for the cognate site and six noncognate sites (WT M.HhaI, black; H127A/T132A M.HhaI, gray). Values are from Tables 2 and 3. Error bars are calculated from triplicate measurements of k_{cat} and duplicate measurements of K_D^{DNA}. The enhancement factor represents the noncognate specificity ratio between the mutant and WT, while both specificities are referenced to the cognate site. *: calculation for fold enhancement = $[(k_{cat}^{HTcognate}/K_D^{HTcognate})/(k_{cat}^{HTnoncognate}/K_D^{HTnoncognate})]/[(k_{cat}^{WTcognate}/K_D^{WTcognate})/(k_{cat}^{WTnoncognate}/K_D^{WTnoncognate})]$.

Table 3: H127A/T132A M.HhaI Kinetic and Thermodynamic Constants

	sequence[a]	k_{cat} (s^{-1})	K_D (nM)	k_{cat}/K_D ($s^{-1}M^{-1}$)
cog	GCGC[b]	$3.9 \times 10^{-2} \pm 4.9 \times 10^{-4}$	1.0 ± 0.19	1.2×10^{8} [d]
A1	**A**CGC[c]	$6.6 \times 10^{-5} \pm 5.8 \times 10^{-6}$	200 ± 33	3.3×10^{2}
T1	**T**CGC	$1.0 \times 10^{-5} \pm 2.0 \times 10^{-6}$	1000 ± 220	1.0×10^{1}
C1	**C**CGC	$1.4 \times 10^{-5} \pm 3.3 \times 10^{-6}$	510 ± 140	2.7×10^{1}
A4	GCG**A**	$3.5 \times 10^{-6} \pm 5.0 \times 10^{-7}$	130 ± 32	2.7×10^{1}
T4	GCG**T**	$6.5 \times 10^{-6} \pm 7.5 \times 10^{-7}$	250 ± 35	2.6×10^{1}
G4	GCG**G**	$3.0 \times 10^{-6} \pm 5.0 \times 10^{-7}$	68 ± 12	4.4×10^{1}

[a] 30mer noncognate hemimethylated DNA. [b] Reported by Youngblood et al. (*28*), unmethylated 30mer; $k_{chem} = 0.12 \pm 0.01$ s^{-1}. [c] K_D^{DNA} by fluorescence anisotropy = 230 ± 41 nM for only noncognate T1; all other K_D^{DNA} values were determined by gel-shift analysis. [d] k_{chem} rate used to determine value.

DISCUSSION

The molecular basis of sequence-specific DNA modification is only partially accounted for by direct protein−DNA contacts, often revealed through structural studies of the enzyme−DNA complex involving a cognate DNA substrate (*40*−*44*). Moreover, the stability and interconversion of reaction intermediates can affect specificity, yet the underlying protein−DNA interactions are difficult to probe by structural studies alone (*10*, *45*−*47*). We suggest that an understanding of such interactions and their contribution toward specificity is essential to the redesign of enzyme specificity, particularly for enzymes which sequence-specifically modify DNA. Indeed, the relative lack of success, in spite of extensive efforts, of rationally redesigning this group of enzymes or devising biomimetic catalysts may be due to the lack of such understanding (*48*).

Wild-Type M.HhaI Specificity toward Noncognate DNA Substrates. Past studies of DNA methyltransferases have identified and characterized specific protein−DNA interactions thought to contribute to sequence recognition (*16*, *18*, *20*−*22*). Surprisingly, no such quantitative analysis is available for M.HhaI, the DNA cytosine methyltransferase which has been exhaustively characterized at the structural level (*13*, *14*, *49*, *50*). Furthermore, little is known about the underlying mechanisms involving induced fit processes leading to target recognition and methylation. Because the various cocrystal structures involving M.HhaI provide atomic resolution images of the protein−DNA interface, we determined the enzyme's binding and catalytic specificity with a subset of noncognate sites, involving substitutions at the first and fourth base pairs (Figure 2C). At the level of k_{cat}/K_M^{DNA}, reduced specificity is found for noncognate substrates ranging from 3000-fold (A1) to 87000-fold (G4) compared to the cognate sequence (Table 2). Changes in specificity constants for the single base substitutions arise from both a decrease in the rate of chemistry and changes in K_M^{DNA}. Changes in the specificity ratio k_{cat}/K_D^{DNA} range from 9000-fold (C1) to 90000-fold (G4) compared to the cognate sequence (Figure 2C and Table 2). k_{cat}/K_D^{DNA} constants for the noncognate substrates are 5−50-fold higher than the k_{cat}/K_M^{DNA} constants for the same noncognate substrate (Table 2). The larger Michaelis constants compared to the DNA dissociation constants suggest that a significant portion of M.HhaI's specificity arises from steps after binding, which may include conformational changes involving the enzyme, substrate, or

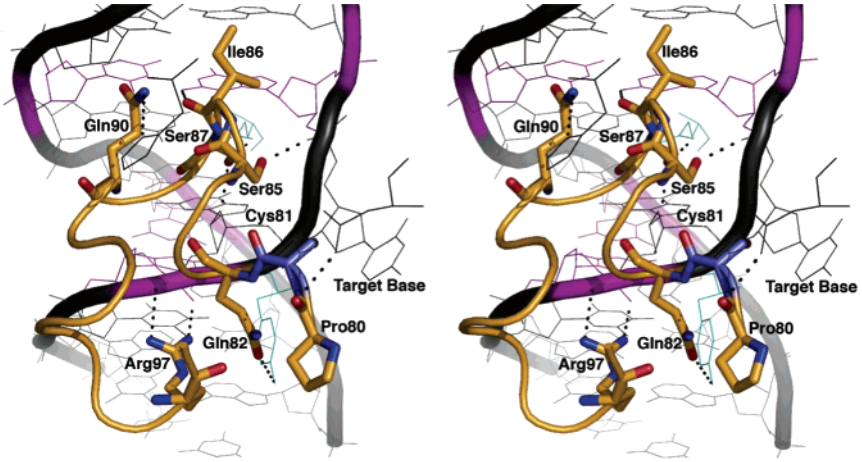

FIGURE 3: Stereoview of the WT M.HhaI flexible loop (residues 80−99, orange) and bound DNA (PDB ID 3MHT). All polar contacts of the loop are shown with dashed lines (up to 3.5 Å between the hydrogen bond partner) to the phosphate backbone, the recognition sequence, and residues of the small domain (cyan). Base pairs 1 and 4 are colored magenta; the nucleophilic residue C81 is colored blue.

both. The discrimination against noncognate sites by M.HhaI revealed here is similar to a prior specificity study of the DNA adenine methyltransferase M.EcoRI (*22*), which also rely at least in part on conformational changes to facilitate noncognate discrimination (*51*).

Reconciling Specificity and Structural Data. We recently obtained a high-resolution cocrystal structure of the wild-type M.HhaI−DNA−AdoHcy complex (1.95 Å), which provides a structural context to understand the quantitative dissociation constants for various noncognate sites and specificity in general (*52*). This structure is nearly identical to the previously reported lower resolution structure (*15*), with subtle alterations involving the orientation of the flipped out target base (*52*). The structure shows that direct DNA contacts involve both protein domains, as well as more indirect interactions with the phosphate−sugar backbone. Ile86 within the flexible loop (residues 80−99) provides main chain-mediated hydrogen-bonding contacts to G1 of the target sequence (Figure 3). Ser87 contacts G3, while other loop residues provide DNA sugar−phosphate backbone contacts with the recognition sequence (Figure 3), suggesting that the flexible loop is directly involved in the recognition of the canonical DNA site. Support for this is provided by our tritium exchange and kinetic isotope experiments examining M.HhaI's ability to methylate poly(dG-dC) and poly(dI-dC) substrates (*16*). This work showed that hydrogen-bonding interactions between loop residue Ile86 and the 2-amino moiety of G1 within the target sequence are important for retaining the extrahelical cytosine in its catalytic pocket (*16*). Thus, both prior structural and kinetic analysis of M.HhaI have suggested a coupling between the flanking nucleotides of the target base and extrahelical positioning of the target base/loop closure (*15*, *16*). How the flanking nucleotides affect target base positioning/loop closure remains to be quantitatively assessed and provides the motivation for the work presented here.

The inability of structurally identified protein−DNA interactions to account for enzymatic specificity has been described for several enzymes (*53*, *54*). Similarly, our specificity results are only partially accounted for by the interactions between the enzyme and its cognate DNA observed in the complex. We recently provided experimental evidence that both loop motion and base flipping contribute toward M.HhaI specificity (*28*) (Estabrook et al., in press). In support of conformational changes playing a role in methyltransferase specificity, we previously demonstrated that replacing His235 with asparagine in the DNA adenine methyltransferase M.EcoRI results in the mutant being impaired in both DNA bending and base flipping (*21*). Importantly, the mutant is dramatically more specific than the wild-type M.EcoRI (*21*), caused largely by the enhanced partitioning of the H235N M.EcoRI−DNA intermediate away from the catalytic complex (*51*). The enhanced specificity results with H127A/T132A M.HhaI (Figure 2C) support the idea that changes in conformational transitions contribute to enzyme specificity. Recently, a similar coupling of DNA recognition and catalysis was proposed for the *Eco*RI endonuclease (*55*). An energetic coupling between catalysis and the ability of certain DNA sequences to undergo a "kinking" transition was proposed to account for the enzyme's fidelity (*55*).

The specificity analysis presented here with naturally occurring DNA sequences provides a direct measure of the enzyme's ability to function with biologically relevant DNA. However, this approach for the most part does not allow the direct assignment of energetics to individual protein−DNA contacts, which is only possible with unnatural base analogues (*54*). Interestingly, on the basis of the cocrystal structure (Figure 4A) the A1 substrate disrupts the interaction between Arg240 and the exocyclic oxygen of guanine 1 and is anticipated to leave other protein−DNA interactions unperturbed (Figure 4A). The ~300-fold loss in affinity (K_D^{DNA}, Table 2) resulting from this substitution with WT M.HhaI corresponds to an ~3.4 kcal/mol loss in binding energy, as would be estimated for the loss in the single hydrogen bond to Arg240 (Figure 4A). However, the 20000-fold difference in the specificity constant (k_{cat}/K_D^{DNA} calculated from Table 2) between cognate and noncognate A1, equivalent to ~5.8 kcal/mol, suggests that energetic mechanisms beyond those assignable based on the cocrystal structure need to be included in our analysis of methyltransferase specificity. Changes in affinity and catalysis between cognate and noncognate substrates (Tables 2 and 3) show very different trends, further suggesting mechanisms other than direct readout to explain substrate discrimination by M.HhaI.

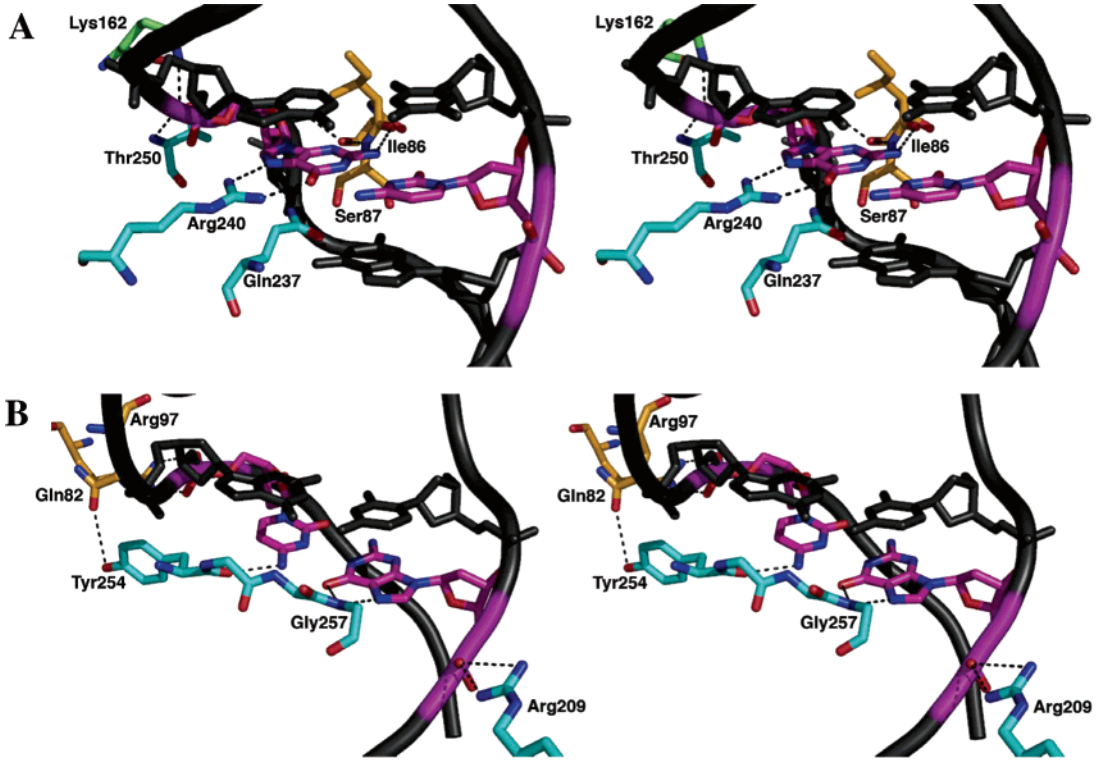

FIGURE 4: Atomistic view of M.HhaI's interaction with base pairs 1 and 4. (A) Stereoview of WT M.HhaI base pair 1 (magenta) (PDB ID 3MHT). Hydrogen bonds to the base pair are shown with dashed lines, loop residue Ile86 is shown in yellow, small domain residues are shown in cyan, and backbone binding of Lys162 in in green. (B) Stereoview of WT M.HhaI base pair 4 (magenta). Hydrogen bonds to the base pair are shown with dashed lines, loop residues Lys89 and Arg97 are shown in yellow, and small domain residues are shown in cyan.

Our prior work, both with M.HhaI and with other DNA methyltransferases, suggests that substrate-dependent conformational rearrangements of the enzyme as well as the DNA can contribute to enzyme specificity (*15*, *17*, *24*). For M.HhaI, we suggest that intermediates involved in stabilizing the extrahelical base, mediated in part by the flexible loop, contribute to just such a mechanism. Loop residue Ser87 interacts with Gln237, and Gln82 interacts with Tyr254 only when the enzyme is bound to DNA; these interactions connect the flexible loop and the protein's small domain interactions with the DNA (*18*, *19*) (Figure 4). The population of the "closed loop" intermediate, forming part of the active site with residues Gln82, Cys81, and Pro80, is much greater upon binding the cognate DNA (Figure 1A) vs noncognate (Estabrook and Reich, in press) (*15*, *17*, *24*). This closed loop intermediate causes the sulfur of Cys81 to become poised for nucleophilic attack at the C6 carbon of the flipped out base (*50*, *56*). Since the correct positioning of Cys81 is critical for catalysis (*50*, *57*, *58*), the conformational change in the flexible loop presents an ideal intermediate which could affect or even direct the specificity of the enzyme. Further, loop residue Ile86 contacts guanine 1 in the target sequence, and Ser87 partially fills the void left in the duplex DNA by the extrahelical positioning of the target base, thereby stabilizing the target base in the active site. Thus, loop positioning, extrahelical base stabilization, and catalysis are likely to be coupled (Estabrook and Reich, in press) (*28*) (Figure 3).

Several studies have recently focused on M.HhaI's conformational changes and the changes in the stability of these reaction intermediates in reference to their potential roles in specificity; similar specificity mechanisms have been proposed for other enzymes (*10*, *21*, *53*). Using computational methods, MacKerrell and co-workers predicted that the flipping intermediate may play such a role in determining M.HhaI's specificity (*39*, *59*). We suggest that the relative destabilization of reaction intermediates with noncognate substrates contributes to the 9000−90000-fold decrease in k_{cat}/K_D^{DNA} by WT M.HhaI compared to the cognate substrate (Table 2 and Figure 2C). The loss of DNA affinity can be accounted for in some cases by the loss of hydrogen-bonding partners between the enzyme and DNA bases, yet the decrease in the rate of catalysis (Table 2) suggests that other unobserved intermediates are perturbed. The loss of a catalytic burst with noncognate substrates (Figure 2A) suggests that the impacted intermediates involve the methylation step or occur prior to this intermediate. Further insight into the structural basis for these changes in intermediate stability awaits the analysis of an M.HhaI−noncognate DNA structure. Nevertheless, changes in the direct readout of the target DNA at the protein−DNA interface mediated through the small domain of the enzyme are likely to be involved. Changes in the indirect readout of the DNA sequence, involving interactions between the flexible loop and the phosphate−sugar backbone, may also be important. Sequence-specific variations in DNA backbone conformations can cause a 1 Å displacement of the phosphate groups in B-DNA (*60*) and have been proposed to contribute to sequence specificity (*54*). Since changes in specificity of the WT enzyme toward noncognate substrates are due to changes in both DNA affinity and the rate of methyl transfer (Table 2), we suggest that DNA affinity is coupled to the placement of catalytic residues. Furthermore, sequence-specific variations of DNA conformation may alter any readout of the substrate by the flexible loop, resulting in both the observed loss of DNA affinity and decreased methyl transfer kinetics

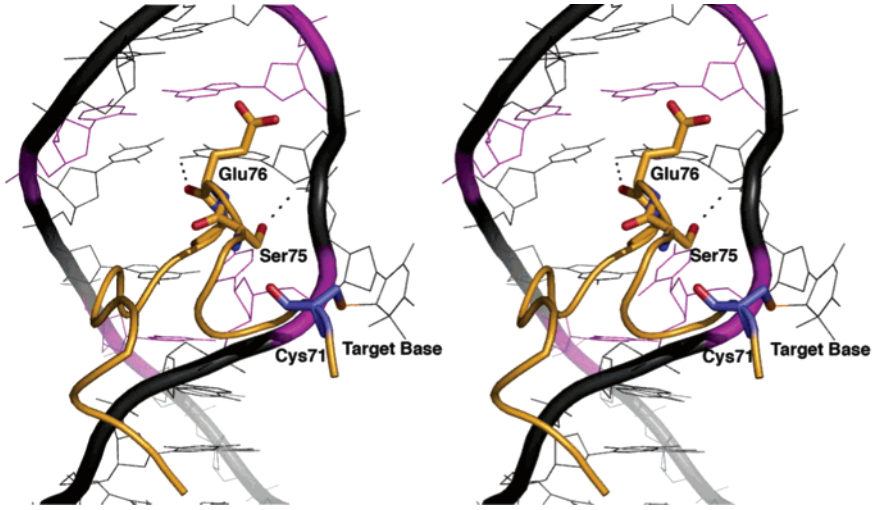

FIGURE 5: Stereoview of M.HaeIII (PDB ID 1DCT). The flexible loop (residues 70−89) is colored yellow, and base pairs 1 and 4 of the target sequence are colored magenta. Hydrogen bonds of the loop residues with base pairs 1, 2, and 4 and contact of the nucleophilic residue Cys71 (blue) with the flipped out cytosine are shown.

observed with the noncognate substrates (Figures 3 and 4). Because elements of the loop directly and indirectly contribute to the correct active site assembly, the enzyme could discriminate against noncognate sites through a DNA-sequence-dependent induction of the correct active site configuration, mediated by the flexible loop (Estabrook et al., in press).

Importance of the Flexible Loop for Recognition. Our specificity results (Table 2 and Figure 2C) of the wild-type M.HhaI and noncognate substrates and prior structural observations of the flexible loop in the "open" conformation in the presence of nonspecific DNA (*17*) suggest that the flexible loop plays an important role in the induced fit mechanism. To probe this, we sought to disrupt the positioning of the loop without making changes within the loop itself. His127 and Thr132 do not directly contact the DNA (Figure 1A), and replacement with alanine was used to disrupt the interface between the flexible loop and the active site of the enzyme. H127A/T132A M.HhaI was chosen for further specificity analysis based on our preliminary determination that the double mutant shows limited changes in the kinetic and thermodynamic constants toward the cognate sequence, while having a severe impact on the same constants for noncognate sequences (*28*).

Rates of methyl transfer for H127A/T132A M.HhaI using noncognate substrates with substitutions in base pair 1 (Figure 1B) are decreased 1800-fold (A1) and up to 12000-fold (T1) relative to the cognate sequence (Table 2 vs Table 3). The methyl transfer ratio ($k_{cat}^{noncognate}/k_{cat}^{cognate}$) for the mutant is 30−70-fold smaller than for WT M.HhaI for noncognate sites modified at base pair 1 (Tables 2 and 3 and Figure 2A) and 3.3−25-fold lower ratios of the corresponding dissociation constants ($K_D^{cognate}/K_D^{noncognate}$) (Tables 2 and 3). Comparisons between WT and H127A/T132A M.HhaI specificity were done by examining $WT^{cognate/noncognate}$ vs $H127A/T132A^{cognate/noncognate}$. Changes in both $k_{cat}^{noncognate}$ and $K_D^{noncognate}$ contribute to the H127A/T132A M.HhaI specificity enhancements of 340-fold (T1) and 460-fold (C1) (Figure 2C). The more conservative substitution A1 yields a smaller specificity enhancement of ∼20-fold for H127A/T132A M.HhaI relative to the WT enzyme (Figure 2C). A specificity enhancement is also observed for H127A/T132A M.HhaI with substitutions in base pair 4, caused in part by 18000-fold (T4) to 40000-fold (G4) decreases in the rate of methyl transfer (Tables 2 and 3). Compared to the WT enzyme, substitutions at base pair 4 cause a 70−180-fold slower rate of methyl transfer for H127A/T132A M.HhaI, while the change in affinity is only 1−10-fold.

The specificity analysis of H127A/T132A M.HhaI supports the hypothesis that the positioning of the flexible loop contributes to the enzyme's induced fit specificity mechanism (Table 3 and Figure 2C). Ile86 lies within the flexible loop and contacts the DNA minor groove, making a direct interaction with the guanine in the GC base pair 1 (**G**CGC) (Figure 3) (*16*, *60*); because other loop elements (Gln82, Cys81, Pro80) in part form the active site, changes between Ile86 and the DNA are likely to impact both DNA affinity and catalysis. Similarly, Arg97, also in the flexible loop, interacts with the DNA phosphate backbone between guanine 3 and cytosine 4 (Figures 2C, 3, and 4B). Protein−DNA interactions involving such backbone moieties are known to contribute to sequence recognition (*1*). Interestingly, we observe 30-, 59-, and 180-fold specificity increases for substrates G4, T4, and A4, respectively, with H127A/T132A M.HhaI compared to WT M.HhaI for the same substrates (Figure 2C). On the basis of examination of the binary and ternary crystal structures of M.HhaI, we suggest that this increased specificity derives from the disruption of the Arg97−DNA interactions which occur during noncognate site modification. The further disruption of the closed loop positioning/stability by the mutation of residues H127A/T132A amplifies the destabilizing effect of the Arg97 interactions with noncognate sites, resulting in a greater loss of binding energy and methylation kinetics. In sum, we suggest that the enhanced specificity of H127A/T132A M.HhaI derives from the destabilization of the flexible loop: although the effect is insufficient to disrupt the mutant's binding and methylation of the cognate site, the combination of internal loop destabilization and the disruption of the protein−DNA interface involving the loop with the noncognate sequences results in an improperly assembled active site.

M.HhaI sequence fidelity arises through the coupling of binding, base flipping, and methyl transfer (Figure 2 and

Tables 2 and 3). The specificity data analyses for WT M.HhaI and the H127A/T132A suggest that loop closure couples target recognition with catalysis through sequence-dependent stabilization of the base-flipped complex (Figures 2C and 3). We suggest that the concept of kinetic proofreading provides a framework with which to understand the specificity of the WT M.HhaI as well as the enhanced double mutant. For WT M.HhaI with the cognate site, partitioning of the reaction intermediates favors the flipped base and formation of the covalent intermediate (*16*). When modifying noncognate sites, intermediate partitioning is shifted away from the base-flipped intermediate because of destabilizing protein−DNA interactions involving loop residues and the minor groove of the DNA (Ile86 directly contacts base pair 1, Ser87 interacts with Gln237, and Gln82 interacts with Tyr254 which contacts base pair 4). Because the H127A/T132A double mutant destabilizes this same flexible loop−minor groove interface, the partitioning of reaction intermediates is perturbed during both cognate and noncognate site modification. However, the effect does not result in significant changes during cognate site methylation by the mutant, whereas the altered partitioning with noncognate sequences is more profound, yielding the observed specificity enhancements (Figure 2C). The more pronounced effects with the double mutant and noncognate substrates presumably arise from the additional destabilization of intermediates in which the loop is in the closed conformation.

Conservation of the Recognition Process. Another structurally characterized DNA C5 methyltransferase, M.HaeIII, recognizes the sequence 5′-GGCC-3′. M.HaeIII methylates noncognate sites with a single substitution 10−27-fold less efficiently than the cognate site in terms of k_{cat}/K_M^{DNA} (*4*). Thus, M.HaeIII is at least 100-fold less specific toward noncognate sites when compared to M.HhaI (ref *4* compared to data from this work). Structural analysis of the M.HaeIII−DNA complex and M.HhaI−DNA complex suggests that M.HhaI and M.HaeIII may exploit similar recognition mechanisms. In particular, M.HhaI and M.HaeIII show significant sequence identity within the large domain which contains the flexible loop (*61*). M.HaeIII and M.HhaI show similar direct and indirect contacts with the target recognition sequence (Figures 3 and 5). Reengineering the specificity of M.HaeIII has been attempted by Cohen et al. with an altered catalytic efficiency (k_{cat}/K_M^{DNA}) up to 670-fold toward a noncognate site, while increasing the cognate catalytic efficiency only 10-fold (*3*, *4*). This specificity increase for a noncognate site of M.HaeIII is mainly due to changes in the Michaelis constant. Mutations causing a negligible effect on the catalytic rate of methylation, while greatly affecting K_M^{DNA}, suggest that the positioning of catalytic residues is less perturbed. The data on M.HaeIII and our work on M.HhaI suggest that specificity enhancement for a certain sequence can be achieved through two different strategies of engineering: (1) Binding of a sequence other than the cognate sequence can be improved by mutations changing the direct readout of the target sequence. (2) Specificity enhancement toward the cognate sequence compared to any noncognate sequence may be achieved by loop disruption, emphasizing the direct and indirect readout of the loop which is coupled to catalysis. For further review on direct and indirect readout mechanisms involved in protein−DNA recognition, see ref *54*.

ACKNOWLEDGMENT

We thank Dr. John Perona for careful analysis and critiques of the manuscript.

SUPPORTING INFORMATION AVAILABLE

WT M.HhaI single-turnover analysis. This material is available free of charge via the Internet at http://pubs.acs.org.

REFERENCES

1. Sinden, R. R. (1994) *DNA Structure and Function*, Academic Press, San Diego, CA.
2. Samuelson, J. C., and Xu, S. Y. (2002) Directed evolution of restriction endonuclease BstYI to achieve increased substrate specificity, *J. Mol. Biol. 319*, 673−683.
3. Cohen, H. M., Tawfik, D. S., and Griffiths, A. D. (2004) Altering the sequence specificity of HaeIII methyltransferase by directed evolution using in vitro compartmentalization, *Protein Eng., Des. Sel. 17*, 3−11.
4. Cohen, H. M., Tawfik, D. S., and Griffiths, A. D. (2002) Promiscuous methylation of non-canonical DNA sites by HaeIII methyltransferase, *Nucleic Acids Res. 30*, 3880−3885.
5. Nakatsukasa, T., Shiraishi, Y., Negi, S., Imanishi, M., Futaki, S., and Sugiura, Y. (2005) Site-specific DNA cleavage by artificial zinc finger-type nuclease with cerium-binding peptide, *Biochem. Biophys. Res. Commun. 330*, 247−252.
6. Wang, C. C., and Dervan, P. B. (2001) Sequence-specific trapping of topoisomerase I by DNA binding polyamide-camptothecin conjugates, *J. Am. Chem. Soc. 123*, 8657−8661.
7. Pei, D., Corey, D. R., and Schultz, P. G. (1990) Site-specific cleavage of duplex DNA by a semisynthetic nuclease via triple-helix formation, *Proc. Natl. Acad. Sci. U.S.A. 87*, 9858−9862.
8. Svedruzic, Z. M., and Reich, N. O. (2005) DNA cytosine C5 methyltransferase Dnmt1: catalysis-dependent release of allosteric inhibition, *Biochemistry 44*, 9472−9485.
9. Svedruzic, Z. M., and Reich, N. O. (2005) Mechanism of allosteric regulation of Dnmt1's processivity, *Biochemistry 44*, 14977−14988.
10. Johnson, K. A. (1993) Conformational coupling in DNA polymerase fidelity, *Annu. Rev. Biochem. 62*, 685−713.
11. Donlin, M. J., Patel, S. S., and Johnson, K. A. (1991) Kinetic partitioning between the exonuclease and polymerase sites in DNA error correction, *Biochemistry 30*, 538−546.
12. Jeltsch, A. (2002) Beyond Watson and Crick: DNA methylation and molecular enzymology of DNA methyltransferases, *ChemBioChem 3*, 274−293.
13. Cheng, X., and Roberts, R. J. (2001) AdoMet-dependent methylation, DNA methyltransferases and base flipping, *Nucleic Acids Res. 29*, 3784−3795.
14. Schubert, H. L., Blumenthal, R. M., and Cheng, X. (2003) Many paths to methyltransfer: a chronicle of convergence, *Trends Biochem. Sci. 28*, 329−335.
15. Klimasauskas, S., Kumar, S., Roberts, R. J., and Cheng, X. (1994) HhaI methyltransferase flips its target base out of the DNA helix, *Cell 76*, 357−369.
16. Svedruzic, Z. M., and Reich, N. O. (2004) The mechanism of target base attack in DNA cytosine carbon 5 methylation, *Biochemistry 43*, 11460−11473.
17. O'Gara, M., Zhang, X., Roberts, R. J., and Cheng, X. (1999) Structure of a binary complex of HhaI methyltransferase with *S*-adenosyl-L-methionine formed in the presence of a short nonspecific DNA oligonucleotide, *J. Mol. Biol. 287*, 201−209.
18. Lee, Y. F., Tawfik, D. S., and Griffiths, A. D. (2002) Investigating the target recognition of DNA cytosine-5 methyltransferase HhaI by library selection using in vitro compartmentalization, *Nucleic Acids Res. 30*, 4937−4944.
19. Daujotyte, D., Serva, S., Vilkaitis, G., Merkiene, E., Venclovas, C., and Klimasauskas, S. (2004) HhaI DNA methyltransferase uses the protruding Gln237 for active flipping of its target cytosine, *Structure (Cambridge) 12*, 1047−1055.
20. Vilkaitis, G., Dong, A., Weinhold, E., Cheng, X., and Klimasauskas, S. (2000) Functional roles of the conserved threonine 250 in the target recognition domain of HhaI DNA methyltransferase, *J. Biol. Chem. 275*, 38722−38730.
21. Allan, B. W., Garcia, R., Maegley, K., Mort, J., Wong, D., Lindstrom, W., Beechem, J. M., and Reich, N. O. (1999) DNA

bending by EcoRI DNA methyltransferase accelerates base flipping but compromises specificity, *J. Biol. Chem. 274*, 19269−19275.
22. Reich, N. O., Olsen, C., Osti, F., and Murphy, J. (1992) In vitro specificity of EcoRI DNA methyltransferase, *J. Biol. Chem. 267*, 15802−15807.
23. Malygin, E. G., Lindstrom, W. M., Jr., Schlagman, S. L., Hattman, S., and Reich, N. O. (2000) Pre-steady state kinetics of bacteriophage T4 dam DNA-[N(6)-adenine] methyltransferase: interaction with native (GATC) or modified sites, *Nucleic Acids Res. 28*, 4207−4211.
24. Cheng, X., Kumar, S., Klimasauskas, S., and Roberts, R. J. (1993) Crystal structure of the HhaI DNA methyltransferase, *Cold Spring Harbor Symp. Quant. Biol. 58*, 331−338.
25. Horton, J. R., Ratner, G., Banavali, N. K., Huang, N., Choi, Y., Maier, M. A., Marquez, V. E., MacKerell, A. D., Jr., and Cheng, X. (2004) Caught in the act: visualization of an intermediate in the DNA base-flipping pathway induced by HhaI methyltransferase, *Nucleic Acids Res. 32*, 3877−3886.
26. O'Gara, M., Roberts, R. J., and Cheng, X. (1996) A structural basis for the preferential binding of hemimethylated DNA by HhaI DNA methyltransferase, *J. Mol. Biol. 263*, 597−606.
27. O'Gara, M., Horton, J. R., Roberts, R. J., and Cheng, X. (1998) Structures of HhaI methyltransferase complexed with substrates containing mismatches at the target base, *Nat. Struct. Biol. 5*, 872−877.
28. Youngblood, B., Shieh, F. K., De L.os, R. S., Perona, J. J., and Reich, N. O. (2006) Engineered extrahelical base destabilization enhances sequence discrimination of DNA methyltransferase M.HhaI, *J. Mol. Biol*. (in press).
29. Lindstrom, W. M., Jr., Flynn, J., and Reich, N. O. (2000) Reconciling structure and function in HhaI DNA cytosine-C-5 methyltransferase, *J. Biol. Chem. 275*, 4912−4919.
30. LeTilly, V., and Royer, C. A. (1993) Fluorescence anisotropy assays implicate protein-protein interactions in regulating trp repressor DNA binding, *Biochemistry 32*, 7753−7758.
31. Lakowicz J. R. (1999) *Principles of Fluorescence Spectroscopy*, Publisher, Address.
32. Estabrook, R. A., Lipson, R., Hopkins, B., and Reich, N. (2004) The coupling of tight DNA binding and base flipping: identification of a conserved structural motif in base flipping enzymes, *J. Biol. Chem. 279*, 31419−31428.
33. Sharma, V., Youngblood, B., and Reich, N. (2005) Residues distal from the active site that alter enzyme function in M.HhaI DNA cytosine methyltransferase, *J. Biomol. Struct. Dyn. 22*, 533−544.
34. Fersht, A. (1999) *Structure and Mechanism in Protein Science*, Publisher, Address.
35. Klimasauskas, S., and Roberts, R. J. (1995) M.HhaI binds tightly to substrates containing mismatches at the target base, *Nucleic Acids Res. 23*, 1388−1395.
36. Allan, B. W., Beechem, J. M., Lindstrom, W. M., and Reich, N. O. (1998) Direct real time observation of base flipping by the EcoRI DNA methyltransferase, *J. Biol. Chem. 273*, 2368−2373.
37. Hopkins, B. B., and Reich, N. O. (2004) Simultaneous DNA binding, bending, and base flipping: evidence for a novel M.EcoRI methyltransferase-DNA complex, *J. Biol. Chem. 279*, 37049−37060.
38. Martin, A. M., Sam, M. D., Reich, N. O., and Perona, J. J. (1999) Structural and energetic origins of indirect readout in site-specific DNA cleavage by a restriction endonuclease, *Nat. Struct. Biol. 6*, 269−277.
39. Huang, N., and MacKerell, A. D., Jr. (2005) Specificity in protein-DNA interactions: energetic recognition by the (cytosine-C5)-methyltransferase from HhaI, *J. Mol. Biol. 345*, 265−274.
40. Cao, C., Jiang, Y. L., Stivers, J. T., and Song, F. (2004) Dynamic opening of DNA during the enzymatic search for a damaged base, *Nat. Struct. Mol. Biol. 11*, 1230−1236.
41. Jiang, Y. L., McDowell, L. M., Poliks, B., Studelska, D. R., Cao, C., Potter, G. S., Schaefer, J., Song, F., and Stivers, J. T. (2004) Recognition of an unnatural difluorophenyl nucleotide by uracil DNA glycosylase, *Biochemistry 43*, 15429−15438.
42. Powell, R. M., Parkhurst, K. M., and Parkhurst, L. J. (2002) Comparison of TATA-binding protein recognition of a variant and consensus DNA promoters, *J. Biol. Chem. 277*, 7776−7784.
43. Wu, J., Parkhurst, K. M., Powell, R. M., Brenowitz, M., and Parkhurst, L. J. (2001) DNA bends in TATA-binding protein-TATA complexes in solution are DNA sequence-dependent, *J. Biol. Chem. 276*, 14614−14622.
44. Sapienza, P. J., De la Torre, C. A., McCoy, W. H., Jana, S. V., and Jen-Jacobson, L. (2005) Thermodynamic and kinetic basis for the relaxed DNA sequence specificity of "promiscuous" mutant EcoRI endonucleases, *J. Mol. Biol. 348*, 307−324.
45. Ninio, J. (1975) Kinetic amplification of enzyme discrimination, *Biochimie 57*, 587−595.
46. Hopfield, J. J. (1974) Kinetic proofreading: a new mechanism for reducing errors in biosynthetic processes requiring high specificity, *Proc. Natl. Acad. Sci. U.S.A. 71*, 4135−4139.
47. Rhodes, G. (2000) *Crystallography Made Crystal Clear*, Academic Press, San Diego, CA.
48. Kraut, D. A., Carroll, K. S., and Herschlag, D. (2003) Challenges in enzyme mechanism and energetics, *Annu. Rev. Biochem. 72*, 517−571.
49. Cheng, X., and Blumenthal, R. M. (1996) Finding a basis for flipping bases, *Structure 4*, 639−645.
50. Kumar, S., Cheng, X., Klimasauskas, S., Mi, S., Posfai, J., Roberts, R. J., and Wilson, G. G. (1994) The DNA (cytosine-5) methyltransferases *Nucleic Acids Res. 22*, 1−10.
51. Youngblood, B., and Reich, N. O. (2006) Conformational transitions as determinants of specificity for the DNA methyltransferase EcoRI, *J. Biol. Chem*. (in press).
52. Shieh, F. K., Youngblood, B., and Reich, N. O. (2006) The role of Arg165 towards base flipping, base stabilization and catalysis in M.HhaI, *J. Mol. Biol*. (in press).
53. Hiller, D. A., Rodriguez, A. M., and Perona, J. J. (2005) Non-cognate enzyme-DNA complex: structural and kinetic analysis of EcoRV endonuclease bound to the EcoRI recognition site GAATTC, *J. Mol. Biol. 354*, 121−136.
54. Jen-Jacobson, L. (1997) Protein-DNA recognition complexes: conservation of structure and binding energy in the transition state, *Biopolymers 44*, 153−180.
55. Kurpiewski, M. R., Engler, L. E., Wozniak, L. A., Kobylanska, A., Koziolkiewicz, M., Stec, W. J., and Jen-Jacobson, L. (2004) Mechanisms of coupling between DNA recognition specificity and catalysis in EcoRI endonuclease, *Structure (Cambridge) 12*, 1775−1788.
56. Wu, J. C., and Santi, D. V. (1987) Kinetic and catalytic mechanism of HhaI methyltransferase, *J. Biol. Chem. 262*, 4778−4786.
57. Mi, S., and Roberts, R. J. (1993) The DNA binding affinity of HhaI methylase is increased by a single amino acid substitution in the catalytic center, *Nucleic Acids Res. 21*, 2459−2464.
58. Lau, E. Y., and Bruice, T. C. (1999) Active site dynamics of the HhaI methyltransferase: insights from computer simulation, *J. Mol. Biol. 293*, 9−18.
59. Huang, N., and MacKerell, A. D., Jr. (2004) Atomistic view of base flipping in DNA, *Philos. Trans. R. Soc. London, Ser. A 362*, 1439−1460.
60. Schroeder, S. A., Roongta, V., Fu, J. M., Jones, C. R., and Gorenstein, D. G. (1989) Sequence-dependent variations in the ^{31}P NMR spectra and backbone torsional angles of wild-type and mutant Lac operator fragments, *Biochemistry 28*, 8292−8303.
61. Reinisch, K. M., Chen, L., Verdine, G. L., and Lipscomb, W. N. (1995) The crystal structure of HaeIII methyltransferase convalently complexed to DNA: an extrahelical cytosine and rearranged base pairing, *Cell 82*, 143−153.
62. Schwede, T., Kopp, J., Guex, N., and Peitsch, M. C. (2003) SWISS-MODEL, An automated protein homology-modeling server, *Nucleic Acids Res. 31*, 3381−3385.

BI061414T